Science Press

Trans. Nonferrous Met. Soc. China 17(2007) s55−s59

Transactions of Nonferrous Metals Society of China

www.csu.edu.cn/ysxb/

# EBSD characterization of recrystallization microstructure of cold-swaged Ti-23Nb-0.7Ta-2Zr-O alloy

GUO Wen-yuan(郭文渊), SUN Jian(孙　坚), LI Xiao-ling(李晓玲), WU Jian-sheng(吴建生)

School of Materials Science and Engineering, Shanghai Jiao Tong University, Shanghai 200240, China

Received 15 July 2007; accepted 10 September 2007

**Abstract:** The microstructures of the cold-swaged and recrystallized Ti-23Nb-0.7Ta-2Zr-O (TNTZO) (mole fraction, %) alloy were investigated by electron backscatter diffraction (EBSD). The difference in microstructure, texture and recrystallization process was evaluated between the TNTZO alloy and traditional body centered cubic (bcc) metals. The results show that the cold-swaged TNTZO alloy presents a pronounced〈110〉fiber texture in the axial direction. The recrystallization of the TNTZO alloy is achieved by the nucleation of new grains and the growth of these new grains at the expense of the deformed structure. The TNTZO alloy behaves a very similar way to traditional bcc metals in the features of the microstructure, texture and recrystallization.

**Key words**: titanium alloy; cold-swaged; recrystallization; EBSD; texture

## 1 Introduction

Titanium and its alloys have been widely used in aerospace and biomedical engineering owing to their advantages such as high strength to mass ratio, outstanding corrosion resistance and biocompatibility. During the last decades, the use of biocompatible titanium alloys has become wide in surgery and medicine relevant. Ti-6Al-4V is the most commonly used material for an orthopaedic to date. However, V and Al are toxic elements[1−2] and the elastic modulus of Ti-6Al-4V alloy is still greater than that of human bone[3]. Therefore, many efforts have been made for development of new non-toxic titanium alloys with low elastic modulus and high strength. The $\beta$ type titanium alloy composed of non-toxic elements is recognized as the best candidates for this purpose. Recently, a new multifunctional $\beta$ titanium alloy, Ti-23Nb-0.7Ta-2Zr-O (TNTZO, mole fraction, %), comprising IVa, Va elements and oxygen was developed by SAITO et al[4−5], which has been thought to deform via a unique dislocation-free mechanism involving nano-scale lattice accommodation, and to possess special properties such as super elasticity, super plasticity, super high strength, and Invar and Elinvar properties[6−9]. The TNTZO alloy with these characteristics is more suitable for biomedical applications than Ti-6Al-4V alloy. However, the occurrence of the dislocation-free deformation mechanism is controversial in the literature [10−12]. If the new alloys deform without the aid of dislocations, how does the recrystallization proceed for this kind of new alloys? More detailed studies are still necessary. In this paper, an automated EBSD system was employed to study the microstructural evolution of the cold-swaged TNTZO alloy under different annealing conditions and evaluate the difference in microstructure, texture and recrystallization process between the TNTZO alloy and traditional body centered cubic (bcc) metals.

## 2 Experimental

The as-received material was the round rods of the TNTZO alloy after cold-swaging with 90% reduction in area. Specimens with the dimension of $d$4 mm×5 mm were carefully cut from the rods by wire-cutting machine, and then subjected to a heat treatment in argon atmosphere at 1 093 K for 5 and 30 min, respectively, followed by brine quenching rapidly to obtain partially and completely recrystallized microstructure. The cross-section of the specimens was mechanical ground

**Foundation item:** Project(50571063) supported by the National Natural Science Foundation of China; Project (04JC14054) supported by the Science and Technology Committee of Shanghai Municipal.

**Corresponding author:** SUN Jian; Tel: +86-21-54745593; E-mail: jsun@sjtu.edu.cn

to 5 μm silicon carbide paper finish, and electro-polished in a 6% perchloric acid + 30% butanol + 64% methanol solution at a closed circuit voltage of 30 V. Crystal orientation measurements were performed using EDAX EBSD facilities attached to the JEOL JSM-6460 scanning electron microscope (SEM) operating at 20 kV. A high speed CCD camera (DigiView) for pattern acquisition and TSL OIM analysis software were used. Orientation information was acquired on a hexagonal grid using a step size of 0.1 μm. For generating orientation and grain boundary maps, a grain tolerance angle of 15° was used, which distinguishes the low angle grain boundaries (LAGBs) and high angle grain boundaries (HAGBs). The orientations of grains are shown in inverse pole figure maps.

## 3 Results and discussion

The typical orientation imaging maps (OIMs) for the cold-swaged, partially recrystallized (annealed at 1 093 K for 5 min) and completely recrystallized (annealed at 1 093 K for 30 min) TNTZO alloys are shown in Figs.1−3, respectively. Fig.1(a) shows the image quality (IQ) map, in which the darker area indicates poorer image quality, also means higher internal stress, whereas the brighter area means lower internal stress. Fig.1(b) shows the unique grain color map. In this map, each grain is assigned a color to distinguish it from neighboring grains. Fig.1(c) shows the grain boundary map, in which the gray and dark lines refer to LAGBs and HAGBs, respectively. Fig.1(d) shows the inverse pole figure (IPF) map where the change in color in each grain corresponds to that in crystal orientation.

The TNTZO alloy is at as-soluted and texture free condition before cold-swaging and the microstructure of the alloy is composed of equiaxed $\beta$ grains 50 to 100 μm in size[5,7]. However, after cold-swaging the IQ map in Fig.1(a) shows that the original grain boundaries cannot be distinguished in the microstructure anymore due to the poor quality of acquired Kikuchi patterns induced by the heavy strain in the TNTZO alloy. The corresponding grain boundary map in Fig. 1(c) shows that there are high densities of LAGBs developed by intense deformation in the cold-swaged alloy. Misorientation angles of those LAGBs fall into the range of 2°−15°, which are termed as sub-boundaries. The fine network of sub-boundaries forms bundles of small subgrains in the micron and submicron range. These subgrains have also been referred to as “deformed cells”[13]. The nature of the

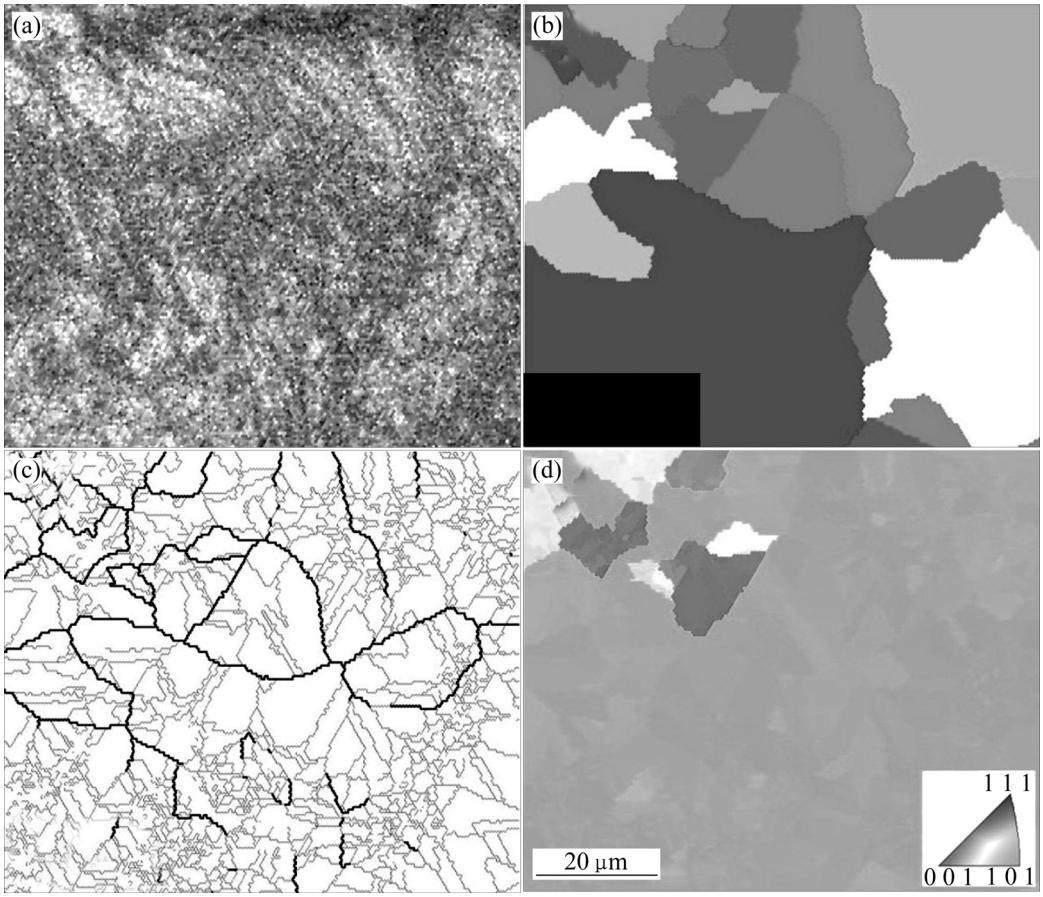


**Fig.1** IQ map (a), unique grain map (b), grain boundary map (c) and IPF map (d) of cold-swaged TNTZO alloy

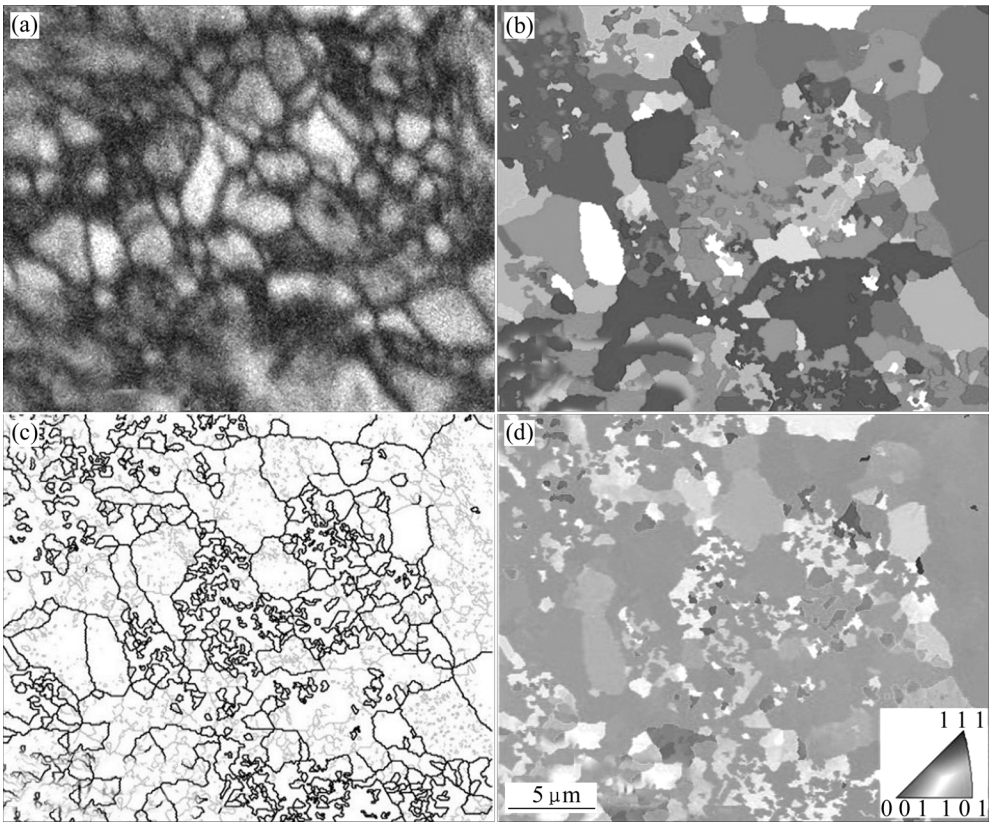


**Fig.2** IQ map (a), unique grain map (b), grain boundary map (c) and IPF map (d) of partially recrystallized TNTZO alloy

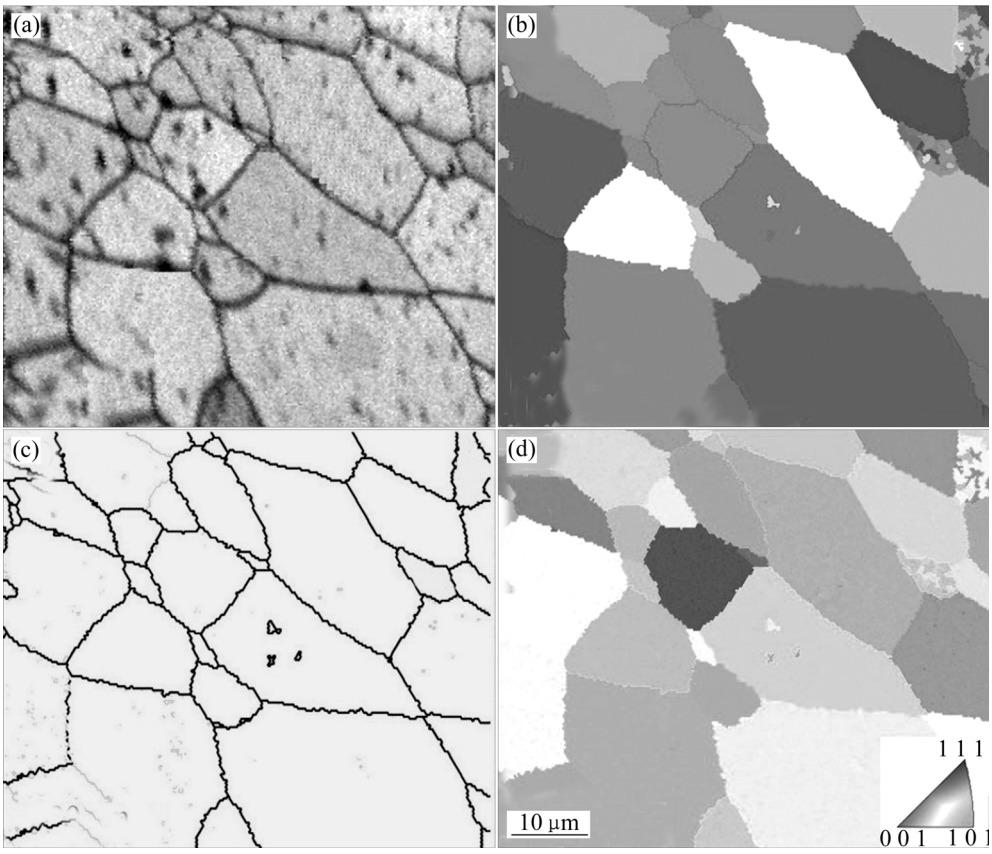


**Fig.3** IQ map (a), unique grain map (b), grain boundary map (c) and IPF map (d) of completely recrystallized TNTZO alloy

substructure developed in the cold-swaged TNTZO alloy varied significantly from one region to another, indicating that individual regions behave quite differently during deformation. The cold-swaged TNTZO alloy presents a predominant 〈110〉 fiber texture in the axial direction, as shown in Fig. 1(d).

The partially recrystallized TNTZO alloy is characterized as a heterogeneous microstructure composed of clusters of coarse structure and fine grains with size of about/less than 1 μm which can be defined as the recrystallized and recovered regions, respectively, as shown in Fig.2. These fine grains are newly recrystallized grains. The distributions of the LAGBs and HAGBs are not homogeneous over the microstructure, with the HAGBs mainly located in the recrystallized regions and the LAGBs mainly in the recovered regions. The 〈110〉 fiber texture parallel to the axial direction is still the predominant texture, whereas the recrystallized grains show different orientation compared to the deformed structure, as shown in Fig.2(d).

After annealing at 1 093 K for 30 min, EBSD analysis shows that complete recrystallization takes place, giving rise to a fairly uniform equiaxed grain structure, where the LAGBs have almost entirely disappeared. The corresponding IPF map of the TNTZO alloy in Fig.3(d) shows that the major texture components become diffused after complete recrystallization and thus no recrystallization texture forms in the TNTZO alloy.

The formation of the marble-like structure in the cold-swaged TNTZO alloy is thought to be associated with the appearance of the deformation band [7]. During cold swaging, large amount of lenticular deformation bands firstly appear in the coarse equiaxed grains of the TNTZO alloy at low deformation degree. With increasing reduction ratio, more deformation bands appear and these bands gradually bend. After 90% cold swaging, the marble-like structure forms in the TNTZO alloy. This marble-like structure appears similar to the "curly grain" or "swirled" structures that commonly found in transverse sections of bcc metals heavily deformed either by wire-drawing or by rotary swaging process[14]. Generally, wire-drawing or rotary swaging produces a pronounced fibrous 〈110〉 texture in traditional bcc metals. The swirled structures result from the fact that plane strain deformation is a favorable strain path for bcc metals developing 〈110〉 textures through the multiple glide or double glide of dislocations along 〈111〉{110}, {112} or {123} systems under tensile dominated applied stress [15]. In order to accommodate this plane strain path, the grains curl about themselves as the diameter of the rod or wire decreases, effectively forming ribbon shapes in three dimensions. The formation of 〈110〉 texture is also predicted for materials with 〈111〉 slip systems by polycrystal plasticity simulations based on plasticity models such as Taylor-Bishop-Hill [16]. In the present study, the texture results of the cold-swaged TNTZO alloy clearly indicate a pronounced 〈110〉 texture. So it is virtually inconceivable that a dislocation-free deformation mechanism could produce this 〈110〉 texture.

It is thought that the sub-boundaries in Fig. 1(c) correspond to those deformation bands in the cold-swaged TNTZO alloy. TEM observations revealed that there are large amount of dislocations in the recovered TNTZO alloy, which is thought to be produced by intense deformation. The detail will be reported elsewhere. Therefore, it is inferred that those sub-boundaries appeared in the cold-swaged TNTZO alloy are dislocation pile-ups. The heterogeneous microstructure indicates that recovery and recrystallization occur simultaneously in the partially recrystallized TNTZO alloy.

The recrystallization of the TNTZO alloy is achieved by the nucleation of new grains, and then these new grains grow at the expense of the deformed structure. The primary recrystallization nuclei possess a different orientation from the deformed structure. Therefore, with increasing the annealing time, the number of recrystallization nucleus gradually increases and some nuclei begin growing, and resultant diffused orientation of the alloy is obtained. This recrystallization process of the TNTZO alloy makes no distinct difference in contrast with that of ordinary bcc metals. As discussed above, the TNTZO alloy behaves similarly to traditional bcc metals in the features of the microstructure, texture and recrystallization progress. These results appear to disagree with the specific dislocation-free plastic deformation mechanism proposed by SAITO et al and GUTKIN et al. So it seems that the TNTZO alloy deforms by the traditional dislocation glide on slip systems, rather than the dislocation-free deformation mechanism.

## 4 Conclusions

1) The deformed structure of the cold-swaged TNTZO alloy is characterized to be of high density of LAGBs. The deformed texture is a distinctive 〈110〉 fiber texture in the axial direction, which is consistent with that of ordinary bcc metals.

2) Primary recrystallization nuclei possess different orientations compared to the deformed structure. After complete recrystallization, the LAGBs have almost entirely disappeared and no recrystallization texture forms in the TNTZO alloy. The recrystallization process

of the TNTZO alloy is also similar to that of ordinary metals.

## References


[1] WALKER P, LEBLANC J, SIKORSKA M. Effects of aluminum and other cations on the structure of brain and liver chromatin[J]. Biochemistry, 1989, 28(9): 3911−3915.

[2] RAO S, USHIDA T, TATEISHI T, OKAZAKI Y, ASAO S. Effect of Ti, Al, and V ions on the relative growth rate of fibroblasts (L929) and osteoblasts (MC3T3-E1) cells[J]. Biomed Mater Eng, 1996, 6(2): 79−86.

[3] KURODA D, NIINOMI M, MORINAGA M, KATO Y, YASHIRO T. Design and mechanical properties of new $\beta$ type titanium alloys for implant materials[J]. Materials Science and Engineering A, 1998, 243(1): 244−249.

[4] SAITO T, FURUTA T, HWANG J, KURAMOTO S, NISHINO K, SUZUKI N, CHEN R, YAMADA A, ITO K, SENO Y, NONAKA T, IKEHATA H, NAGASAKO N, IWAMOTO C, IKUHARA Y, SAKUMA T. Multi functional titanium alloy “GUM METAL”[J]. Materials Science Forum, 2003, 426(4): 681−688.

[5] SAITO T, FURUTA T, HWANG J, KURAMOTO S, NISHINO K, SUZUKI N, CHEN R, YAMADA A, ITO K, SENO Y, NONAKA T, IKEHATA H, NAGASAKO N, IWAMOTO C, IKUHARA Y, SAKUMA T. Multifunctional alloys obtained via a dislocation-free plastic deformation mechanism[J]. Science, 2003, 300(5618): 464−467.

[6] HWANG J, KURAMOTO S, FURUTA T, SAITO T. Phase-stability dependence of plastic deformation behavior in Ti-Nb-Ta-Zr-O alloys[J]. Journal of Materials Engineering and Performance, 2005, 14(6): 747−754.

[7] FURUTA T, KURAMOTO S, HWANG J, NISHINO K, SAITO T. Elastic deformation behavior of multi-functional Ti-Nb-Ta-Zr-O alloys[J]. Materials Transaction, 2005, 46(12): 3001−3007.

[8] GUTKIN M, ISHIZAKI T, KURAMOTO S, OVID’KO I. Nanodisturbances in deformed gum metal[J]. Acta Materialia, 2006, 54(9): 2489−2499.

[9] KURAMOTO S, FURUTA T, HWANG J, NISHINO K, SAITO T. Plastic deformation in a multifunctional Ti-Nb-Ta-Zr-O alloy[J]. Metallurgical and Materials Transactions A, 2006, 37(3): 657−662.

[10] KIRITANI M. Dislocation-free plastic deformation under high stress[J]. Materials Science and Engineering A, 2003, 350(1/2): 1−7.

[11] KIRITANI M, SATOH Y, KIZUKA Y, ARAKAWA K, OGASAWARA Y, ARAI S, SHIMOMURA Y. Anomalous production of vacancy clusters and the possibility of plastic deformation of crystalline metals without dislocations[J]. Philosophical Magazine Letters, 1999, 79(10): 797−804.

[12] SCHIØTZ J, LEFFERS T, SINGH B. Dislocation nucleation and vacancy formation during high-speed deformation of fcc metals[J]. Philosophical Magazine Letters, 2001, 81(5): 301−309.

[13] COLLINGS E. The physical metallurgy of titanium alloys[M]. Metals Park, OH: American Society for Metals, 1984: 172.

[14] HOSFORD W. Microstructural changes during deformation of [011] fiber-textured metals[J]. Trans TMS-AIME, 1964, 230: 12−15.

[15] GORELIK S. Recrystallization in metals and alloys[M]. AFANASYEV V transl. Moscow: MIR Publishers, 1981: 57, 307, 371.

[16] ARIS S, PYZALLA A, REIMERS W. Simulation of the development of deformation textures and residual stresses using the Taylor-Bishop-Hill theory[J]. Computational Materials Science, 1999, 16(1/4): 76−80.


**(Edited by ZHAO Jun)**